Supplemental Material for "Observation of Flat Frequency Bands at Open Edges and Antiphase Boundary Seams in Topological Mechanical Metamaterials"

Kai Qian,[1] Linghua Zhu,[2] Keun Hyuk Ahn,[1] and Camelia Prodan[1]

[1] *Department of Physics, New Jersey Institute of Technology, Newark, New Jersey, USA*
[2] *Department of Physics, Virginia Tech, Blacksburg, Virginia, USA*

I. THEORETICAL ANALYSIS

In this section, further details of the theoretical analysis are provided. As described in Ref. [S1], the normalized Lagrangian for two magnetically coupled spinners is approximately given by

$$\begin{aligned}\frac{L(\varphi_1,\varphi_2,\dot{\varphi}_1,\dot{\varphi}_2)}{2\pi^2 I} =& \frac{1}{4\pi^2}\dot{\varphi}_1^2 + \frac{1}{4\pi^2}\dot{\varphi}_2^2 - \frac{1}{2}\alpha(\varphi_1^2+\varphi_2^2) \\ & - \beta\varphi_1\varphi_2,\end{aligned} \tag{S1}$$

where I represents the moment of inertia of each spinner, φ_1 and φ_2 the rotation angles of the two spinners from the equilibrium states. The parameters α and β represent the coefficients in potential energy terms and depend on the strengths of the magnets attached at the end of spinner arms and the distance between the magnets. If we represent the parameter β for the spinner pairs connected by the blue, red, and green lines in Fig. 1(b) in the main text as β_b, β_r, and β_g, the condition for the gap opening is $\beta_g < (\beta_b+\beta_r)/2$, under which the system becomes topological if $\beta_b < \beta_r$ and nontopological if $\beta_b > \beta_r$. For the topological insulator spinner systems, the parameter values are $\beta_b = 106.7\ \mathrm{Hz}^2$, $\beta_r = 280.0\ \mathrm{Hz}^2$, and $\beta_g = 83.4\ \mathrm{Hz}^2$.

Applying periodic boundary conditions in the n_2 direction, the localization length $\xi(k_2)$ for the edge states with the wave vector k_2 is found to be

$$\xi(k_2) = \frac{4}{\ln\frac{\beta_r^2+\beta_g^2+2\beta_r\beta_g\cos k_2}{\beta_b^2+\beta_g^2+2\beta_b\beta_g\cos k_2}}, \tag{S2}$$

similar to the localization length for the 1D SSH system [S2]. The amplitude of the oscillation for the left-edge state with the wave vector k_2 decays as

$$A_{k_2}(n_1,n_2) = \begin{cases} Ae^{-(n_1-1)/\xi(k_2)} & \text{for odd } n_1 \\ 0 & \text{for even } n_1 \end{cases} \tag{S3}$$

and for the right-edge state as

$$B_{k_2}(n_1,n_2) = \begin{cases} 0 & \text{for odd } n_1 \\ Be^{-(N_1-n_1)/\xi(k_2)} & \text{for even } n_1 \end{cases} \tag{S4}$$

in the limit of the large edge-to-edge distance, N_1. With the parameter values given above for the topological spinner systems, we obtain the localization length $\xi(k_2)$ versus k_2 as shown in Fig. S1, with $\xi(k_2)$ ranging between 0.9 at $k_2 = \pm\pi$ and 3.1 at $k_2 = 0$ in the unit of the spinner-to-spinner distance. The above theoretical results are used to analyze the experimental results shown in Figs. 4(e) and 4(f) in the main text.

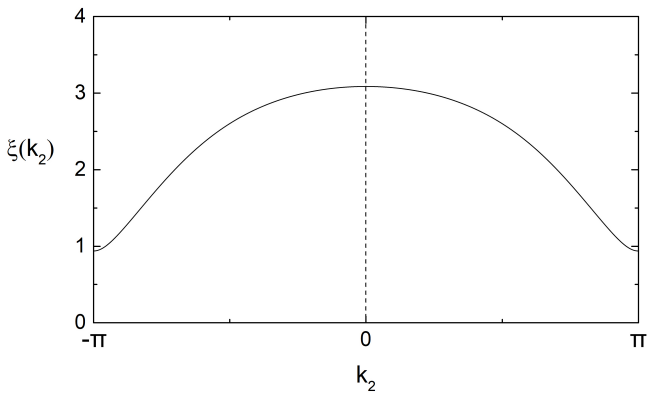

FIG. S1. Localization length $\xi(k_2)$ versus the edge state wave vector k_2 in the limit of the large edge-to-edge distance N_1 for the topological spinner systems. $\xi(k_2)$ varies between 0.9 at $k_2 = \pm\pi$ and 3.1 at $k_2 = 0$.

The frequency splitting $\Delta f(k_2)$ between the two edge modes with the wave vector k_2 is $\Delta f(k_2) = CN_1e^{-N_1/\xi(k_2)}$ in the limit of large $N_1/\xi(k_2)$. Since the localization length $\xi(k_2)$ is largest at $k_2 = 0$, the edge band width Δf_0 is given by

$$\Delta f_0 = CN_1e^{-N_1/\xi_0} \tag{S5}$$

in the limit of large N_1/ξ_0, where $\xi_0 = \xi(k_2 = 0)$, the localization length at $k_2 = 0$. The plot of $\ln(\Delta f_0)$ versus N_1 for experimental data is fitted into $\ln(\Delta f_0) = \ln C + \ln N_1 - N_1/\xi_0$ to estimate ξ_0, as shown in Fig. 2(l) in the main text.

II. ADEQUACY OF THE CHOSEN SPINNER SYSTEM SIZES

In this section, the sizes experimentally chosen for the spinner systems are shown to be adequate to demonstrate the flatness of the edge bands. Since Fig. 2(k) in the main text demonstrates that experimental results agree well with numerical simulations for the edge band width, numerical simulations with open boundary conditions are used for the analysis.

First, for the $N_1 \times N_2$ spinner system, we fix N_1 to 4, 6, 8, 10, and 12, the values chosen for the experiments,

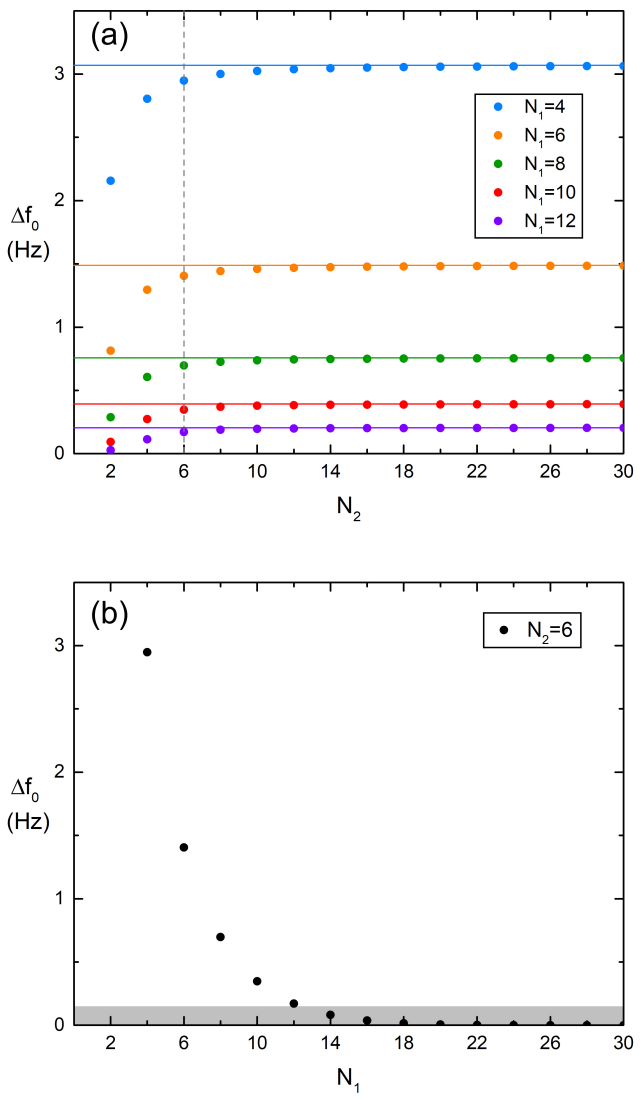

FIG. S2. (a) Symbols: Edge band width Δf_0 versus N_2, calculated for $N_1 \times N_2$ systems with $N_1 = 4$, 6, 8, 10, and 12 and open boundary conditions. Horizontal solid lines: Δf_0 calculated for $N_2 = 1{,}000$ as a large N_2 limit for each case of N_1. Vertical dashed line: $N_2 = 6$ chosen for experimental setups. (b) Edge band width Δf_0 versus N_1, calculated for the $N_1 \times 6$ systems with open boundary conditions. The gray area approximately represents the experimental resolution, below which the edge band width cannot be measured reliably.

and varies N_2 up to 1,000 to see how the edge band width Δf_0 depends on N_2. The results in Fig. S2(a) show that the edge band width Δf_0 increases as N_2 increases. The values of Δf_0 at $N_2 = 1{,}000$, which could be considered as the large N_2 limit, are shown as horizontal lines. The results show that the edge band widths Δf_0 at $N_2 = 6$ (vertical dashed line), the size chosen for experimental setups for the results in Fig. 2 in the main text, are only about $0.12 \sim 0.03$ Hz, or $5 \sim 15\%$ smaller than the corresponding large N_2 limits for the systems with $N_1 =$ 4, 6, 8, 10, and 12, which indicates that the choice $N_2 =$ 6 is adequate. Relatively quick saturation of Δf_0 for N_2 as small as 6 in Fig. S2(a) is consistent with the edge band width being determined at $k_2 = 0$ [See Eq. (S5)], which is insensitive to the number of k_2-points.

Next, with N_2 fixed at 6, we examine how adequate the experimental choice of $N_1 = 4$, 6, 8, 10, 12 is to represent the trend in the edge band width Δf_0 versus N_1. The results in Fig. S2(b) show that the edge band width Δf_0 continues to decrease as the edge-to-edge distance N_1 increases further up to 30, and becomes below the experimental resolution, shown in gray area, beyond around $N_1 = 12$. Rapid decrease of the edge band width with the increase in N_1 from $N_1 = 4$ to 12 reflects the relatively short localization length, $\xi(k_2) = 0.9 \sim 3.1$ in the unit of spinner-to-spinner distance for the chosen experimental parameters. The experimental results for $N_1 = 6$, 8, 10, and 12 also allow us to reveal exponential decrease of the edge band width Δf_0 with respect to N_1, consistent with the theoretical predictions, as shown in Fig. 2(l) in the main text. Therefore, our choice of $N_1 =$ 4, 6, 8, 10, 12 and $N_2 = 6$ for experimental setups is adequate to show that the edge band would have a vanishing width and become flat in the whole projected reciprocal space in the limit of large edge-to-edge distance.

[S1] D. J. Apigo, K. Qian, C. Prodan, and E. Prodan, Topological edge modes by smart patterning, Phys. Rev. Mater. **2**, 124203 (2018).

[S2] J. K. Asbóth, L. Oroszlány, and A. Pályi, *A Short Course on Topological Insulators: Band structure and edge states in one and two dimensions* (Springer, Cham, 2016).